Conditions for reliable time-resolved dosimetry of electronic portal imaging devices for fixed-gantry IMRT and VMAT

Inhwan Jason Yeo[a)]
Department of Radiation Medicine, Loma Linda University Medical Center, Loma Linda, California 92354

Jae Won Jung
Department of Physics, East Carolina University, Greenville, North Carolina 27858

Baldev Patyal and Anant Mandapaka
Department of Radiation Medicine, Loma Linda University Medical Center, Loma Linda, California 92354

Byong Yong Yi
Department of Radiation Oncology, University of Maryland School of Medicine, Baltimore, Maryland 21201

Jong Oh Kim
Department of Radiation Oncology, University of Pittsburgh Cancer Institute, Pittsburgh, Pennsylvania 15232

(Received 24 December 2012; revised 3 May 2013; accepted for publication 28 May 2013; published 17 June 2013)

Purpose: The continuous scanning mode of electronic portal imaging devices (EPID) that offers time-resolved information has been newly explored for verifying dynamic radiation deliveries. This study seeks to determine operating conditions (dose rate stability and time resolution) under which that mode can be used accurately for the time-resolved dosimetry of intensity-modulated radiation therapy (IMRT) beams.
Methods: The authors have designed the following test beams with variable beam holdoffs and dose rate regulations: a 10 × 10 cm open beam to serve as a reference beam; a sliding window (SW) beam utilizing the motion of a pair of multileaf collimator (MLC) leaves outside the 10 × 10 cm jaw; a step and shoot (SS) beam to move the pair in step; a volumetric modulated arc therapy (VMAT) beam. The beams were designed in such a way that they all produce the same open beam output of 10 × 10 cm. Time-resolved ion chamber measurements at isocenter and time-resolved and integrating EPID measurements were performed for all beams. The time-resolved EPID measurements were evaluated through comparison with the ion chamber and integrating EPID measurements, as the latter are accepted procedures. For two-dimensional, time-resolved evaluation, a VMAT beam with an infield MLC travel was designed. Time-resolved EPID measurements and Monte Carlo calculations of such EPID dose images for this beam were performed and intercompared.
Results: For IMRT beams (SW and SS), the authors found disagreement greater than 2%, caused by frame missing of the time-resolved mode. However, frame missing disappeared, yielding agreement better than 2%, when the dose rate of irradiation (and thus the frame acquisition rates) reached a stable and planned rate as the dose of irradiation was raised past certain thresholds (a minimum 12 s of irradiation per shoot used for SS IMRT). For VMAT, the authors found that dose rate does not affect the frame acquisition rate, thereby causing no frame missing. However, serious inplanar nonuniformities were found. This could be overcome by sacrificing temporal resolution (10 frames or 0.95 s/image): the continuous images agreed with ion chamber responses at the center of EPID and the calculation two-dimensionally in a time-resolved manner.
Conclusions: The authors have determined conditions under which the continuous mode can be used for time-resolved dosimetry of fixed-gantry IMRT and VMAT and demonstrated it for VMAT.
 [http://dx.doi.org/10.1118/1.4811099]

Key words: electronic portal imaging device, continuous mode, step and shoot, sliding window, volumetric intensity modulated arc delivery

I. INTRODUCTION

An electronic portal imaging device (EPID) is an onboard, transit imager that has been used for dose validation.[1–7] The integration mode (IM) of image acquisition in EPID, built to acquire all beam outputs without synchronization to beam pulses, has mostly been used in such applications. Recently, a continuous scanning mode (CM) has been investigated by McCurdy and Greer.[8] Unlike IM, CM was designed to acquire beam pulses synchronously. They validated CM, in spite of potential frame losses, by comparing two-dimensional (2D) CM images after summation with IM images. Evaluating time-resolved dosimetry, the authors additionally compared CM images with time-resolved ion chamber (IC) measurements at a central (ctr) point. Their work did not evaluate the time-resolved dosimetry two-dimensionally, which

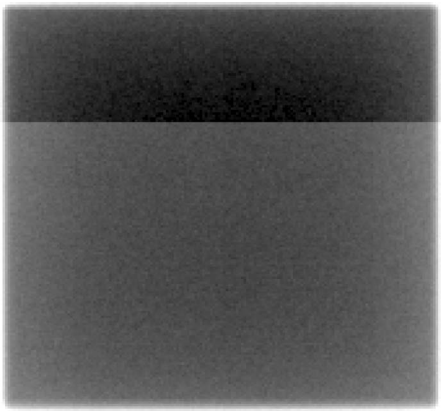

FIG. 1. A frame image from continuous scan of VMAT with SW delivery.

we believe is necessary for the successful two-dimensional dosimetric performance of CM. Continuous imaging benefits dynamic delivery techniques because it can provide information about not only beams but also internal organs, although in a limited manner, thus potentially validating four-dimensional delivery techniques.

The image acquisition of EPID is sequential and time-dependent. In a time period of one frame acquisition (i.e., ~0.1 s), the dose (pulse) rate can change, thereby affecting the profile of the image (see Fig. 1). Time-resolved image acquisition can then be influenced by the temporal variability in intensity-modulated radiation therapy (IMRT) that utilizes dose rate modulations such as step and shoot (SS) and sliding window (SW) techniques. Note that the two delivery techniques are different in dose rate modulation, even if the same amount of dose is delivered. Volumetric modulated arc therapy (VMAT) adds gantry rotation to an exiting IMRT beam, wherein the gantry rotation can provide an additional constraint to dose rate modulation.[9] The aforementioned temporal nature of EPID image acquisition can therefore be affected by such differences in the IMRT techniques.

Therefore, the objective of this study is to determine suitable operating conditions (dose rates and time resolution) of EPID for time-resolved dosimetry of IMRT beams. This evaluation includes using (1) VMAT and fixed-gantry IMRT beams with SW delivery and additionally the latter with SS delivery; (2) continuous as well as integration modes in terms of EPID acquisition while the latter serves as a standard reference; and (3) pointwise as well as planar evaluations. This new study for time-resolved dosimetry validation of CM investigates planar response of CM images and determines operable beam and EPID conditions.

II. METHODS

To achieve the objectives, we have designed test beams (SS, SW, and VMAT); measured them on EPID and an ion chamber; calculated EPID response to a VMAT beam; and evaluated the measurements and calculations.

II.A. Test beam design

The test beams are as follows: (1) A 10 × 10 cm open, non-IMRT beam was made. (2) A SW beam was made by utilizing the motion of a pair of multileaf collimator (MLC) leaves outside the 10 × 10 cm jaw opening (Fig. 2). The pair with a 0.5 cm opening was programmed to move between −5 and +5 cm with five repetitions. (3) For the SS beam, the same pair was programmed to move discontinuously with the same extent of movement. (4) A VMAT beam was designed by adding gantry movement to the SW field from 180° to 0°. Due to machine limitations, only three repeat movements were programmed. The test beams were designed in such a way that beam holdoffs and dose rate regulations were variable among the four beams and among the deliveries of various monitor units (MUs) assigned to each, while delivering the same total dose under the same field opening (10 × 10 cm^2). Various MUs for the two dose rates, 300 and 600 MU/min, were assigned based on dose rate fluctuations associated with each MU for each beam, as the fluctuations affect the response of EPID. If the fluctuations appeared around a certain dose level, MUs were sampled in small steps around the dose level to determine such threshold MU. In addition, representative MUs from lower and higher dose ranges than the threshold were selected. By using these conditions which are representative of various IMRT beams in their characteristics of dose rate modulation, their outputs on the CM of EPID can be clearly studied while the open beam serves as a reference.

In addition to the above, for 2D, time-resolved evaluation, we have designed a VMAT beam with X1 MLC travel from

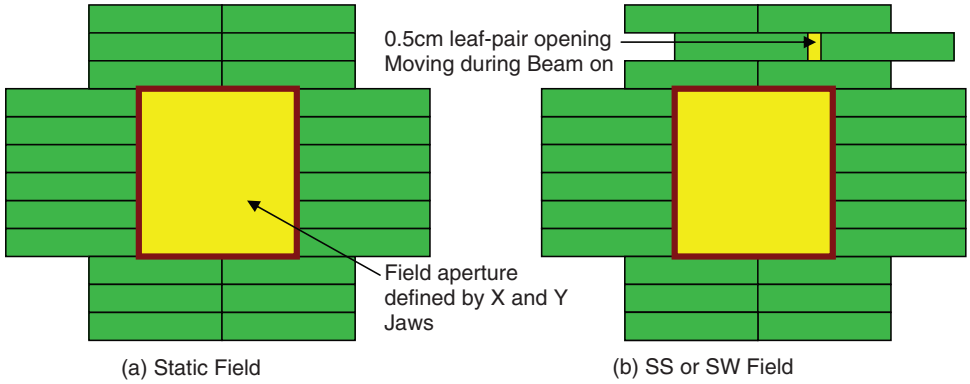

FIG. 2. (a) Static and (b) IMRT beams.

−5 to 2 cm and back (one cycle) with three repetitions over the gantry rotation from 180° to 0°, while X2 MLC is fixed at 5.5 cm and Y opening at 10 cm (beam no. 5). An amount of MU (300 MU at 300 MU/min) was assigned, such that a stable dose rate could be assumed during delivery and EPID image sorting did not have to involve frame rounding off with a frame acquisition rate of 10 frames/s. Therefore, during each 20 s interval, the MLC travelled one cycle; the gantry rotated through 60°; 200 frames were acquired.

II.B. Measurement: EPID

Each beam was irradiated on EPID (IDU20), positioned 150 cm from the target. The irradiated EPID operated in CM and IM. As a standard procedure, dark and flood fields were measured and used to correct images. For the image acquisition, a frame acquisition rate of approximately 10.50 frames/s was assigned. For image acquisition, BeamOnDelay and FrameStartDelay were set as 0 to capture all beam pulses from the beam. Trigger delay (synchronization delay, a waiting time between the beam pulse capture and the start of row scanning) was set at 6 milliseconds (ms), a default number in the system. LineStartDelay (delay until each row scanning starts) was set as 2 ms, also a default number.

For each MU irradiation, we have not only acquired EPID images, but also manually recorded frame number and frame acquisition rate that appear in the image acquisition window, associated with each image (due to actual dose rate fluctuations, they were different from the planned). For each acquisition, three repeated measurements were performed.

As our measurements involved irradiations under fluctuating dose rate, characterized by various test beams, we also tested the impact of dose rate variations on CM images. Dark and flood field calibrations were performed at 300 MU/min, and CM images from the open beam (27.2 × 20.8 cm that covers the entire EPID at 150 cm) of 50 MU were measured at 100, 200, 300, and 400 MU/min, while the flood field calibration was at 300 MU/min.

II.C. Measurement: Ion chamber

Integrating ion chamber measurements were performed for all test beams with various MUs (amounts used in EPID measurements) to confirm the integrity of test beam deliveries. To validate the temporal performance of EPID for SW and VMAT deliveries, time-resolved ion chamber measurements were performed. For both measurements, an ion chamber (Xradin farmer chamber A12, Standard Imaging, Inc.) was used under a 1.2 cm-thick build-up cap.

II.D. Evaluation

Acquired CM images were evaluated in terms of measurement reproducibility, dose linearity, and accuracy in central pixel values. The reproducibility requires reproducibility in frame numbers which in turn requires a steady frame acquisition rate. Therefore, the latter was investigated as well. Reproducibility was mathematically defined as "1 − std/mean" where std implies standard deviation of three measured data. Linearity is concerned with the reduction of central pixel value/MU normalized to the value for the maximum MU of irradiation for each beam. Accuracy was so defined to reproduce the open beam output measured in IM, which serves as base calibration for dosimetry applications of images acquired in CM. It is mathematically a ratio of data in this study. The images in IM were also evaluated in the linearity for comparative understanding of the CM images.

CM images were numerically integrated to be compared with IM images. They were additionally compared in a time-resolved manner with the ion chamber measurements. For such evaluations, central pixel values within an area of 0.5 × 0.5 cm were sampled. In order to investigate the appropriateness of 2D CM images for dosimetry, longitudinal profiles across the CM images were evaluated. After this evaluation, a strategy was developed to determine a suitable time resolution that would allow utilization of the CM images for time-resolved dosimetry. With the determined time resolution, 2D time-resolved dosimetry was performed using the measured CM images of the test beam no. 5 to demonstrate their accuracy and usefulness. The CM images were calibrated to calculated EPID images based on our Monte Carlo (MC) model of EPID developed earlier,[6] and compared with the calculated EPID dose images with the determined time resolution.

For all evaluations, the acquired images were imported into and processed in MATLAB (version 7.10 with image processing tool box, Mathworks, Natick, MA). Ion chamber measurements for testing integrity of the test beam deliveries were similarly evaluated for each IMRT beam delivery.

III. RESULTS

III.A. Test beam integrity

Integrating ion chamber measurements for all test beams produced reproducible data within 0.1% and linear data within 0.2%. The minimum accuracy (0.6% error) in generating the non-IMRT open beam output was observed in the output of the VMAT for irradiations at 600 MU/min. This accuracy does not necessarily imply IMRT beam delivery uncertainty, but a limited isocentricity during gantry rotation and the related isocentric difference between the static ion chamber position and the rotating gantry. Therefore, delivery of the test beams was found to be stable and thus suitable for this study. Note that we have tested the beam integrity at isocenter; but EPID acquisition can entail more uncertainties due to its 2D nature.

III.B. EPID image evaluation

To quantify the impact of dose rate fluctuations caused by the use of a fixed flood-field calibration file, the difference in CM images between the irradiations at 300 and 100 MU/min was determined to be 1.2%. That between the irradiations at 300 and 400 MU/min was 2.2% at the center, provided the pixel value profiles were relatively uniform. It is not possible that when the nominal dose rate was at 300 MU/min, the

TABLE I. EPID image evaluation of reproducibility, linearity, and accuracy for dose delivery at 300 MU/min. Frame acquisition rate was 10.59 frames/s, approximately, for all IM. Cells in bold contain data of the irradiation condition that is not acceptable for use of CM.

Irradiation condition			Integration mode ctr pixel	Continuous mode (sync) Frame	ctr pixel		
	MU	MU/min	Linearity	Frame/s	Reproducibility (%)	Linearity	Accuracy
Open	50	300	0.995	10.59	99.478	0.983	0.986
	100		1.000		…	…	…
	120		0.999	10.59	99.936	0.996	0.996
	130		1.000		…	…	…
	190		1.000		…	…	…
	380		1.001		…	…	…
	400		1.000	10.59	99.953	1.000	0.998
SW	50	100–130[a]	1.000	**4.3**	**99.490**	**0.163**	**0.163**
	120	270–300[a]	0.998	**10.20–10.59**[b]	**99.825**	**0.925**	**0.923**
	130	300	0.998	10.59	99.917	0.994	0.991
	400	300	1.000	10.59	99.883	1.000	0.997
SS	50	300	0.998	**4.15**	**96.314**	**0.858**	**0.846**
	380		1.000	**4.15–10.59**[c]	**99.266**	0.999	**0.978**
	400		1.000		99.989	1.000	0.981
VMAT	50	80–85	0.999	10.59	99.930	0.997	0.995
	190[d]	300	1.000	10.59	99.951	1.000	0.993

[a]Lower dose rate appeared at the turn of MLC motion direction.
[b]10.59 during MLC motion and 10.20 at the turn of MLC motion direction: this corresponds to the dose rate change.
[c]Initial buildup of frame acquisition rate is involved due to dose rate ramping up at the start up of shooting after each step.
[d]From 190 MU and above, the dose rate becomes stable and reaches the prescribed rate.

fluctuation will alter the dose rate to 400 MU/min. Actual error is expected to be much less than 1.2%.

Table I shows measurement data of ctr pixel value and their evaluation parameters with varying monitor units from the acquisition in IM and CM of irradiations at 300 MU/min. Table II shows similar data for irradiations at 600 MU/min. For brevity, only the frame acquisition rate was listed because it is critical for acquisition of time-resolvable frames. In this section, dosimetric imaging with CM was validated by comparing (1) postintegrated CM images with IM images,

TABLE II. EPID image evaluation of reproducibility, linearity, and accuracy for dose delivery at 600 MU/min. Frame acquisition rate was 10.50 frames/s, approximately, for all IM. Cells in bold contain data of the irradiation condition which is not acceptable for use of CM.

Irradiation condition			Integration mode ctr pixel	Continuous mode (sync)x Frame	ctr pixel		
	MU	MU/min	Linearity	Frame/s	Reproducibility (%)	Linearity	Accuracy
Open	100	600	0.999	10.59	99.960	0.981	0.983
	190		1.001	10.48–10.73	99.814	0.994	0.993
	240		1.001			…	…
	250		1.001			…	…
	380		1.001			…	…
	400		1.001			…	…
	1100		1.001			…	…
	1200		1.000	10.59	99.924	1.000	1.001
SW	100	207–318[a]	1.000	**4.23–4.54**	**96.400**	**0.168**	**0.168**
	240	550–600[a]	0.999	**10.25–10.59**[b]	**99.322**	**0.923**	**0.918**
	250	600	1.000	10.46–10.81	99.954	0.998	0.994
	400	600	1.000	10.59	99.855	1.000	0.996
SS	100	600	0.999	**2.58–4.15**	**96.531**	**0.852**	**0.839**
	1100		1.000	**4.15–11.2**[c]	**99.602**	0.995	**0.979**
	1200		1.000	4.15–10.59[c]	99.879	1.000	0.984
VMAT	100	148–172	0.998	10.59	99.958	0.997	0.996
	380[d]	600	1.000	10.59–10.81	99.967	1.000	0.996

[a]Lower dose rate at the turn of MLC motion direction.
[b]10.59 during MLC motion and 10.2 at the turn of MLC motion direction; this corresponds to the dose rate change.
[c]Initial buildup of frame acquisition rate is involved due to dose rate ramping up at the start up of shooting after each step.
[d]From 380 MU and above, the dose rate becomes stable and reaches the prescribed rate; note that this is twice of 190 MU associated with 300 MU/min.

(2) time-resolved CM images with time-resolved ion chamber measurements, and (3) time-resolved CM images with time-resolved EPID image calculations.

III.B.1. Integrating dosimetry

III.B.1.a. Using integration mode. Although IM is a well-documented mode of acquisition, we have summarized the results for comparison with CM and to discuss new findings.

SW, SS, and VMAT beams: In IM, the linearity in ctr pixel values was found to be within 1%–2% for all dose levels, dose rates, and types of beams. This finding on acquisition of IM is different from our earlier finding on the nonlinearity of IM for acquisition of the SS beam (i.e., for 10 MU/shoot at 300 MU/min, the nonlinearity was greater than 2%).[11] The earlier finding was based on an aS500 system. Vial *et al.*[10] have also reported the nonlinearity of greater than 2% in EPID pixel values for MUs under 20 when irradiated by an open beam of 10×10 cm^2. They have attributed such nonlinearity to image lag and ghosting effects occurring within the first seconds from onset of irradiation. Our study differed: we were concerned with IMRT beams with dose rate fluctuations in the middle of irradiation.

III.B.1.b. Using continuous mode without temporal resolution. SW beam: Acquired images in CM were summed and evaluated in comparison with IM. For the SW beam, the evaluation parameters in ctr pixel value were found to be greater by 1%–2% than their expected values when frame acquisition rate was not maintained steadily or close to the planned rate (bold data in Tables I and II). Lower or fluctuating frame acquisition rates imply frame missing occurrence during acquisition, thereby contributing to the above poor parameters. This condition was provided when dose rate fluctuated by 5% on an average (270–300 from 300 MU/min). From the trend of the neighboring data and the fluctuated dose rates associated with each irradiation that caused such fluctuations, however, it is proper to interpret that any dose fluctuation is hardly tolerated to achieve acceptable linearity. Unlike IM, the trend of the frame acquisition rate of CM depended on that of the dose rate because CM is synchronized to beam pulses. Observed frame missing (frame n linearity not reported for brevity) is from a difference source and reason than those reported previously.[8] Dose rate irregularity during irradiation (not at beginning or end) caused frame missing.

SS beam: For the SS beam, the evaluated parameters were greater than 2% for the same reasons as those for the SW beam. This is represented in the poorer evaluation parameters associated with the delivery of lower MUs (bold data in Tables I and II). While the above explanations based on fluctuating dose and frame acquisition rates similarly apply, for the SS beam dose rate ramping-up at the start of each shoot additionally affected the frame acquisition, as shown by the fluctuating frame acquisition rates (see column frame/s, Table I) with the lower rate associated with dose rate ramping-up (e.g., 4.15 than 10.59 during the shoot).

Tables I and II also show that the parameters approached to within 2%, if minima of 400 and 1200 MU (40 and 120 MU per shoot) were used for 300 and 600 MU/min, respectively. These numbers correspond to the irradiation duration of 8 and 12 s per shoot for 300 and 600 MU/min, respectively. As the delivery duration associated with the fluctuations (dose rate ramping up) decreased relatively (when MUs increased), more stable acquisition without missing frames was achieved on EPID. The minima determined for SW and SS beams can depend on MLC movement patterns that affect delivered dose rates and their fluctuations as well as temporally variable linac beam characteristics.

VMAT beam: For the VMAT beam, unlike fixed-gantry IMRT beams, the parameters evaluated for EPID performance in ctr pixel value were all within 1% for the two dose levels (low and high) and dose rates, as shown in Tables I and II. In spite of fluctuating dose rates, the frame acquisition rate was steady and at the planned level, causing no frame missing. Such performance characteristic in the acquisition of CM for VMAT is promising for time-resolved dosimetry.

III.B.2. Time-resolved dosimetry

III.B.2.a. Using continuous mode with time resolution. SW beam: Figure 3 shows time-resolved EPID (1 frame/image) measurement at central axis of EPID compared with IC measurements at isocenter for fixed-gantry IMRT with SW delivery of 130 MU at 300 MU/min. This condition (beam and MU) was chosen because it offered reliable CM acquisition, affected by stable dose rate, that provided a steady time resolution needed for time-resolved dosimetry. It showed good agreement of CM images with the acquired, time-resolved IC signals, demonstrating the low noise of time-resolved EPID dosimetry.

VMAT beam and temporal resolution adjustment: For VMAT, CM images were found to have longitudinal nonuniformities (Fig. 1). Such a pattern is present in arc delivery such as VMAT, although it can appear in other unstable EPID acquisition where significant pulse modulation is involved. The impact of this nonuniformity is represented in Figs. 4(a) and 4(b) which show temporal fluctuations at the center of

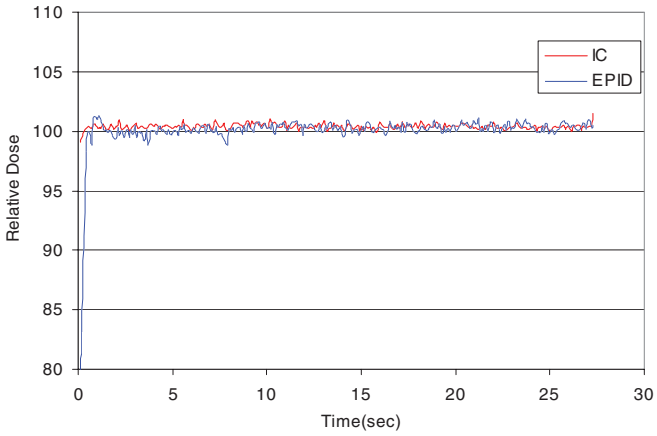

FIG. 3. Temporal EPID (1 f/image) vs IC measurements for fixed-gantry IMRT (130 MU) with SW delivery at 300 MU/min. The dose rate of irradiation was steady around 300 MU/min.

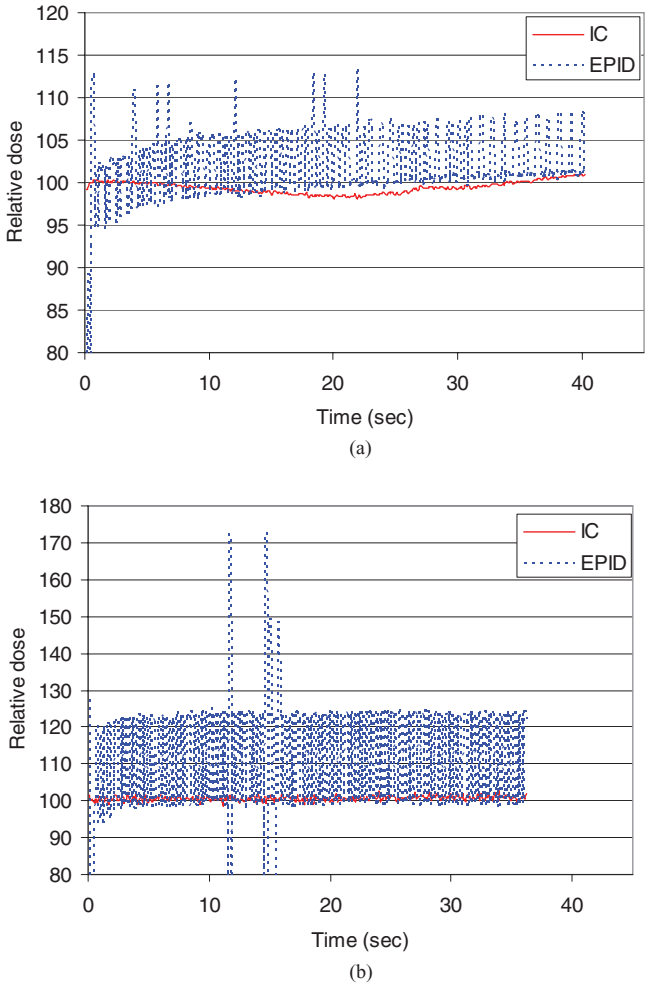

FIG. 4. Temporal EPID (1 f/image) vs IC measurements for VMAT [(a) 190 MU; (b) 50 MU] with SW delivery at 300 MU/min.

EPID while IC is steady, causing time-resolved EPID dosimetry impossible. In spite of the nonuniformity, the many frames of CM images were reported to produce a uniform image close to that of IM when summed up.[8] We have confirmed this in Sec. III.B.1.b. This can be explained by the sufficiently random occurrence of such nonuniformities across the inplane direction, given that each frame captures many pulses, such as 17 pulses/frame, and CM images contain a large number of frames (close to 400 in this study). Although necessary for the application of CM for dosimetry, such agreement alone does not qualify it for time-resolved dosimetry because such frames with spatial nonuniformities do not represent the real irradiated beam which is uniform across the beam aperture.

With the objective of still utilizing CM images, we can hypothesize that if nonuniformities are sufficiently randomly distributed, sacrifice in time resolution, by assigning multiframes to a single image, may produce an acceptably uniform image for dosimetry applications. To test this hypothesis, we summed ten frames to generate a single image (i.e., 0.95 s/image), which provided acceptable uniformity. We have determined this number after iterative trials. For the 50 MU case at 300 MU/min, we have calculated 3%, 3%, and 5% maximum uniformity, respectively, for three sets of images from

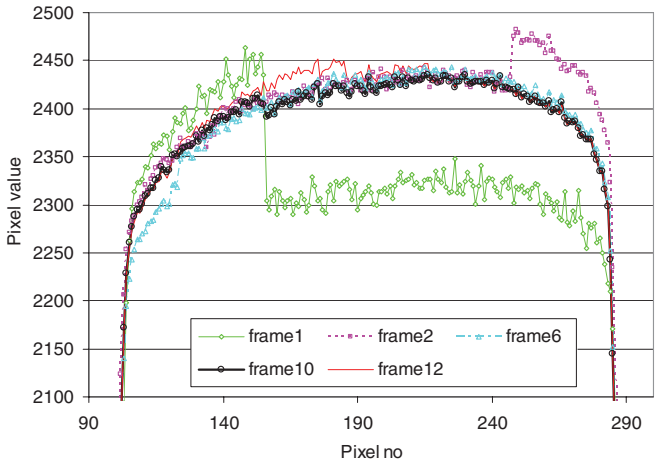

FIG. 5. Intercomparison among inplane pixel profiles of summed-averaged frames over 1, 2, 6, 10, and 12 frames. 190 MU was used at 300 MU/min. The central pixel number is 192.

three separate irradiations (each image contains ten frames). For the 190 MU case, similar outcomes were 3%, 2%, and 2%. For the 100 MU case at 600 MU/min, uniformity was 3% for all three irradiations: for 380 MU, it was 2% for all three. Uniformity was defined as (fractional standard deviation or std)/(mean of the pixel values) enclosed within the central 80% of the irradiated areas. Results were considered acceptable, given that a typical EPID image showed maximum 2% uniformity according to our calculation.

Figure 5 displays the gradual improvement of the inplanar uniformity by frame averaging as the frame number to be averaged increased for the case of 190 MU. The uniformity reached the acceptable level by averaging over ten frames. Figure 6 shows the validation of the dosimetric response of CM images by comparing temporal EPID (0.95 s/image) measurement with temporal IC measurements for VMAT delivery. It shows that the temporal fluctuation in EPID images was reduced, thus matching the temporal IC response to within 2.5% for the case of the 190 MU irradiation where the dose rate was stable; to within +3/−3.5% for the 50 MU irradiation where the dose rate was highly fluctuating and reduced from the nominal rate (see Table I). A part of IC response fluctuation was due to the potential misplacement of IC from the isocenter by the amount of laser alignment error and the limitations in the isocentricity (gantry sagging and a finite rotational isocenter radius). Figure 6 demonstrates confidence in the EPID dosimetry using CM after the temporal resolution adjustment. This was possible by not only frame averaging, but also steady frame acquisition, in spite of dose rate fluctuations, that offered steady time resolution without frame missing.

Figure 7 shows profiles of time-resolved EPID images with MC calculations; among ten phases, five temporal phases were selected to be displayed. The figure shows agreements when MLCs travel from X1 to X2 directions (i.e., the initial programmed direction of travel). For all ten phases with the exception of the first phase (0.5 s), the gamma pass rates were above 97%, given 3 mm distance to agreement and 3% dose

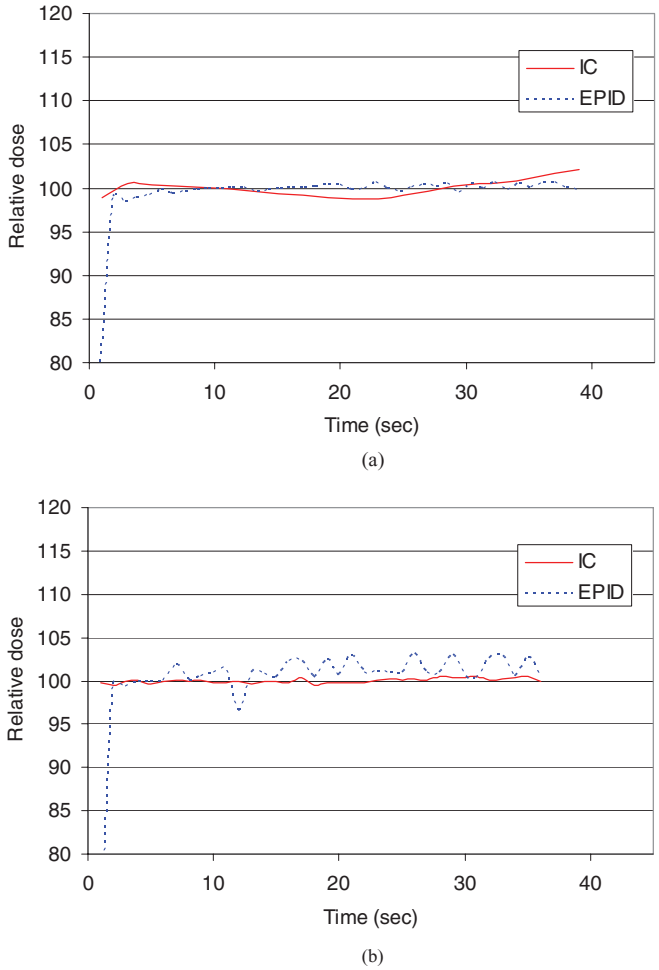

FIG. 6. Temporal EPID (10 f/image) vs IC measurements for VMAT [(a) 190 MU; (b) 50 MU] with SW delivery at 300 MU/min. Frame averaging (0.95 s for an image) was performed.

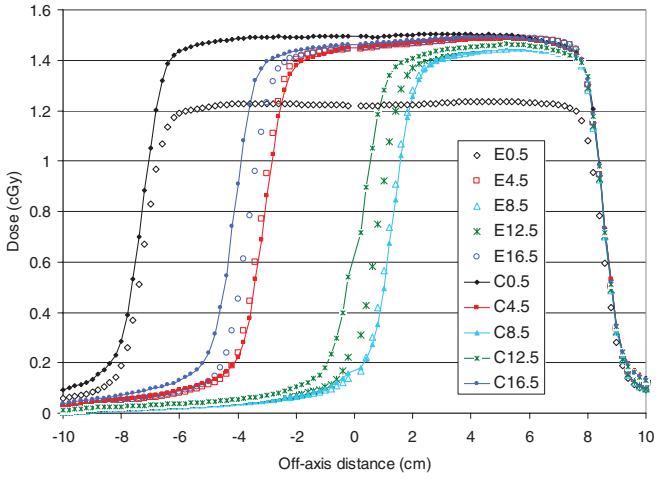

FIG. 7. Profile comparison of time-resolved EPID (10 f/image) measurements with the corresponding calculations for VMAT with SW delivery (test beam no. 5) of 300 MU at 300 MU/min. Frame averaging (1 s for an image) was performed. E0.5: EPID profile at 0.5 s; C: Calculation. The figure shows comparison of selected temporal phases for the radiation delivery carried out during the first cycle of MLC movements (60°).

difference (DD). The disagreement in DD of the first phase is due to dose rate ramping up at the start of irradiation to which EPID measurements respond while the calculation could not. When MLCs travel back, after they have reached the assigned limit, they showed lagging for all phases (10.5 through 19.5 s) that amounts to 4 mm, approximately. This trend was repeated by the succeeding cycles (2 and 3) and repeated measurements of similar beams. The only difference was that the first phases of second and third cycles showed agreement, unlike that of the first cycle, because the dose-rate ramping up was no longer involved. It is to be noted that in spite of MLC lagging, once MLCs are set to move in the initially programmed motion for the second and third cycles, lagging disappeared. Lagging was reproduced when the collimator was rotated to 90°, eliminating the influence of gravity. Understanding MLC travel is beyond the scope of this study.

IV. CONCLUSION

This study tested the continuous scanning mode of EPID image acquisition for application in time-resolved dosimetry for, in turn, validating VMAT and dynamic delivery techniques. As a result, we found conditions that will allow steady frame acquisition, necessary for associating a time resolution with each image, and dose linearity. They are as follows: (1) For the fixed-gantry IMRT, dose rate fluctuations should not occur or deviate from the nominal rate for sliding-window IMRT and irradiation durations should be greater than 8 and 12 s/shoot for 300 and 600 MU/min, respectively, for step-and-shoot IMRT. To meet these conditions, MUs beyond certain minima have to be assigned to each IMRT beam under measurement; (2) For VMAT, nonuniformity in continuous EPID images must be resolved by sacrificing time resolution, such as 1 s/image. No frame missing occurs for VMAT, in spite of dose rate fluctuations, offering the acquisition of the EPID images with a steady time resolution. For each clinical beam, however, a time resolution has to be determined that will produce acceptable uniformity.

Accuracy and efficacy of the time-resolved dosimetry were demonstrated through this study. This study opens up follow-up studies about clinical applications of time-resolved EPID dosimetry for arc therapy.

ACKNOWLEDGMENTS

The first author wishes to express appreciation to Eric Eichholz, Daniel Morf, and Peter Munro in Varian Medical Systems, Inc., for their consultation. This study was in part supported by NIH R01CA133539 (PI: Byong Yong Yi).

[a]Author to whom correspondence should be addressed. Electronic mail: medicphys@hotmail.com; Telephone: 909 558 4904.

[1]J. V. Siebers, J. O. Kim, L. Ko, P. J. Keall, and R. Mohan, "Monte Carlo computation of dosimetric amorphous silicon electronic portal images," Med. Phys. **31**, 2135–2146 (2004).

[2]E. Spezi and D. G. Lewis, "Full forward Monte Carlo calculation of portal dose from MLC collimated treatment beams," Phys. Med. Biol. **47**, 377–390 (2002).

[3]C. V. Dahlgren, K. Eilertsen, T. D. Jorgensen, and A. Ahnesjo, "Portal dose image verification: The collapsed cone superposition method applied with different electronic portal imaging devices," Phys. Med. Biol. **51**, 335–349 (2006).
[4]W. Van Elmpt, S. Nijsten, and R. Schiffeleers, "A Monte Carlo based three-dimensional dose reconstruction method derived from portal dose images," Med. Phys. **33**, 2426–2434 (2006).
[5]B. Warkentin, S. Steciw, S. Rathee, and B. G. Fallone, "Dosimetric IMRT verification with a flat-panel EPID," Med. Phys. **30**, 3143–3155 (2003).
[6]J. W. Jung, J. O. Kim, I. J. Yeo, Y. Cho, S. M. Kim, and S. DiBiase, "Fast transit portal dosimetry using density-scaled layer modeling of aSi-based electronic portal imaging device and Monte Carlo method," Med. Phys. **39**, 7593–7602 (2012).
[7]G. Jarry and F. Verhaegen, "Patient-specific dosimetry of conventional and intensity modulated radiation therapy using a novel full Monte Carlo phase space reconstruction method from electronic portal images," Phys. Med. Biol. **52**, 2277–2299 (2007).
[8]B. M. C. McCurdy and P. B. Greer, "Dosimetric properties of an amorphous-silicon EPID used in continuous acquisition mode for application to dynamic and arc IMRT," Med. Phys. **36**, 3028–3039 (2009).
[9]G. Nicolini, A. Clivio, L. Cozzi, A. Fogliata, and E. Vanetti, "On the impact of dose rate variation upon RapidArc® implementation of volumetric modulated arc therapy," Med. Phys. **38**, 264–271 (2011).
[10]P. Vial, P. Greer, L. Oliver, and C. Baldock, "Initial evaluation of a commercial EPID modified to a novel direct-detection configuration for radiotherapy dosimetry," Med. Phys. **35**, 4362–4374 (2008).
[11]I. Yeo, J. Jung, B. Yi, F. Piskulich, D. Choi, P. Nookala, and B. Patyal, "Instability of electronic portal imaging device responses for intensity modulated irradiation," Med. Phys. **38**, 3594 (2011).